

SCIENTIFIC REPORTS



OPEN

Differences in resource use lead to coexistence of seed-transmitted microbial populations

G. Torres-Cortés¹, B. J. Garcia², S. Compant³, S. Rezki¹, P. Jones², A. Prévieux¹, M. Briand¹, A. Roulet⁴, O. Bouchez⁴, D. Jacobson² & M. Barret¹

Seeds are involved in the vertical transmission of microorganisms in plants and act as reservoirs for the plant microbiome. They could serve as carriers of pathogens, making the study of microbial interactions on seeds important in the emergence of plant diseases. We studied the influence of biological disturbances caused by seed transmission of two phytopathogenic agents, *Alternaria brassicicola* Abra43 (Abra43) and *Xanthomonas campestris* pv. *campestris* 8004 (Xcc8004), on the structure and function of radish seed microbial assemblages, as well as the nutritional overlap between Xcc8004 and the seed microbiome, to find seed microbial residents capable of outcompeting this pathogen. According to taxonomic and functional inference performed on metagenomics reads, no shift in structure and function of the seed microbiome was observed following Abra43 and Xcc8004 transmission. This lack of impact derives from a limited overlap in nutritional resources between Xcc8004 and the major bacterial populations of radish seeds. However, two native seed-associated bacterial strains belonging to *Stenotrophomonas rhizophila* displayed a high overlap with Xcc8004 regarding the use of resources; they might therefore limit its transmission. The strategy we used may serve as a foundation for the selection of seed indigenous bacterial strains that could limit seed transmission of pathogens.

Plant-associated microbial assemblages (a.k.a plant microbiome) can impact plant fitness through the modification of a number of traits including biomass production, flowering time or resistance to abiotic and biotic stresses^{1–4}. Due to these important effects on plant growth and health, numerous studies have focused mainly on the microbial communities horizontally acquired from the environment and associated with the rhizosphere and phyllosphere^{5–7}. Although the relative contribution of vertical transmission in the ultimate composition of the plant microbiome is probably limited⁸, vertically-transmitted microorganisms can also have an important impact on plant fitness⁹. For instance, vertically-transmitted microorganisms can promote germination of seeds through the production of cytokinins^{10,11} or increase nutrient availability in shoots and roots¹². A well-documented example of vertical transmission is seed transmission of plant pathogenic agents. Seed transmission of plant pathogens, including viruses, bacteria and fungi, was initially identified in the late 1800s - early 1900s¹³. Seed-transmission of plant pathogenic agents serves as a major means of dispersal and can therefore be responsible for disease emergence and spread^{13,14}. Very low degrees of seed contamination by bacterial pathogens can lead to efficient plant colonization¹⁵. Furthermore, seed transmission of plant pathogens is usually asymptomatic and can take place on non-host plants^{16,17}, which can then serve as a reservoir of plant pathogens.

To control seed transmission of plant pathogens one should either eradicate them on seed-producing crops or perform seed treatments. Fungicide application during plant production or as seed treatment is an effective means of fungal pathogen management¹⁸. Since these chemical-base methods are unsatisfactory for bacterial plant pathogens and have a potentially harmful environmental impact¹⁹, alternative control methods have been proposed, including seed health testing, physical seed treatment (e.g. thermotherapy) and biological methods such as seed coating of specific biocontrol agents^{14,18}. Direct incorporation of biocontrol agents within the seed tissues through inoculation of seed-producing crops is of interest to restrict seed transmission of plant pathogenic agents. Recently, this

¹IRHS, Agrocampus-Ouest, INRA, Université d'Angers, SFR4207 QuaSaV, 49071, Beaucouzé, France. ²Biosciences Division, Oak Ridge National Laboratory, Oak Ridge, Tennessee, USA. ³AIT Austrian Institute of Technology GmbH, Center for Health and Bioresources, Bioresources Unit, Konrad Lorenz Straße 24, A-3430, Tulln, Austria. ⁴INRA, US 1426, GeT-PlaGe, Genotoul, Castanet-Tolosan, France. Correspondence and requests for materials should be addressed to G.T.-C. (email: gloriatorresco@gmail.com)

approach (called EndoSeed™) has been successfully performed by introducing the plant-growth promoting strain *Paraburkholderia phytofirmans* PsJN into seeds of multiple plant species through spray-inoculation of the parent plant at the flowering stage²⁰. Therefore, inoculation of strain(s) that can compete with plant pathogens for resources and space may be of interest to limit seed transmission of phytopathogenic agents²¹.

Although inoculation of biocontrol microorganisms on or within the seeds may improve seedling health by protecting them against seed-borne or soil-borne pathogens, adequate formulation of these microorganisms for a successful seed colonization and subsequent persistence on seedlings is still challenging¹⁸. Further knowledge about the interactions between phytopathogenic agents and other members of the plant microbiome could provide clues on the selection of candidate strains that compete with the target plant pathogen. These microbial interactions can be estimated by analyzing the response of the seed microbiome following seed-transmission of plant pathogens. Indeed, this approach can potentially reveal co-occurrence and more importantly exclusion between plant pathogens and resident members of the seed microbiota²². Recently, we initiated such an approach by studying the response of the radish seed microbiome to seed-transmission of two plant pathogens of brassicas, the bacterial strain *Xanthomonas campestris* pv. *campestris* 8004 (Xcc8004²³) and the fungal strain *Alternaria brassicicola* Abra43 (Abra43^{24,25}). These plant pathogens are frequent seed colonizers of a range of Brassicaceae species including cabbage, cauliflower, turnip and radish^{26,27}. Additionally, they differ in their seed transmission pathways: Xcc8004 being seed-transmitted through the systemic and floral pathways while Abra43 being transmitted through the external pathway^{28–30}.

According to community profiling approaches, seed transmission of Abra43 impacted the taxonomic composition of the fungal fraction of the seed microbiome, while Xcc8004 did not change the structure of the seed microbiota²⁴. The absence of changes in community structure following Xcc8004 seed transmission could be explained by differences in ecological niches between the plant pathogen and the members of the seed microbiome. In this work, we therefore investigated competition for resources (nutrient and space) between Xcc8004 and seed-borne bacterial strains (epiphytes and endophytes) of radish (*Raphanus sativus* var. Flamboyant5) through a combination of metagenomics, metabolic fingerprinting, bacterial confrontation assays, and fluorescence *in situ* hybridization approaches.

Results

Impact of Xcc8004 and Abra43 transmission on the structure of the seed microbiome. The relative abundances (RA) of Xcc8004 and Abra43 within the radish seed microbiome were assessed through mapping of the metagenomic reads against their reference genomic sequences. According to mapping results, Xcc8004 RA increased from 1% of paired-end reads in the control samples to 6% and 30% for X2013 and X2014, respectively (Additional file 1). Abra43 RA increased from 0.1% to 1.1% in 2013 and from 0.02% to 0.58% in 2014 (Additional file 1).

Metagenomic reads were used to predict the structure of the seed microbiome with a modified and parallelized version of Kraken (ParaKraken). The vast majority of the classified reads were derived from two bacterial families: *Erwiniaceae* and *Pseudomonadaceae* (Fig. 1a), while less than 0.06% of reads were classified as *Dikarya* (Additional file 2). At a genus level (Fig. 1g), the seed microbiome was mainly composed of *Pantoea* and *Pseudomonas*. In addition, we detected an increase in the RA of reads affiliated with *Xanthomonas* and to a lesser extent *Alternaria* in seed samples contaminated with Xcc8004 and Abra43, respectively (Fig. 1a,g).

To assess the impact of Xcc8004 and Abra43 transmission on the seed microbiome structure, we first removed the reads affiliated with the species *Xanthomonas campestris* and *Alternaria brassicicola* in the species table generated with ParaKraken. On average, 3,850 species (SD + 385) were detected in seed-associated microbial assemblages collected from control plots (Fig. 1b). This estimation is one order of magnitude higher than the richness predicted with 16S rRNA gene or *gyrB*²⁴. According to Kruskal-Wallis non parametric analysis of variance followed by Dunn's post-hoc test, the observed species richness, the predicted species richness and the species diversity were not significantly affected ($P > 0.01$) by seed transmission of both phytopathogenic agents (Fig. 1b). Differences in community membership and community composition between seed samples were assessed with Jaccard and Bray-Curtis indexes, respectively (Fig. 1e,f). While seed transmission of Xcc8004 and Abra43 did not alter community membership and composition ($P > 0.01$), the harvesting year explained 54.9% ($P = 0.001$) and 62.8% ($P = 0.001$) of variation in community membership and composition, respectively.

Although the overall structure of the radish seed microbiome was not impacted by Xcc8004 and Abra43 seed transmission, we assessed changes in specific taxa RA through fcros³¹ and DUO^{32,33} analyses. High abundance species (>0.1% RA) across all three conditions (i.e., Xcc8004 seed transmission (X), Abra43 seed transmission (A) and control (C)) were compared to identify differentially abundant species (Additional file 3). Of the 35 differentially abundant species across all conditions, 22 (63%) were *Pseudomonas*. DUO of the non-pathogen reads identified two networks with positive associations and no network with negative association (Additional file 4). The two networks were largely split by genus with one network having 67% of interacting species as *Pantoea* and the other with 67% of *Pseudomonas*. Both genera were predominant in the seed microbiome. None of the abundant species had a DUO score of >0.75, also suggesting that these pathogens had no major impact on the structure of the microbiome.

Functional composition of the seed microbiome. Taxonomic profiling of the seed microbiomes has shown no significant differences in the community structure between samples harvested from control plots and plots inoculated with Xcc8004 and Abra43. As genomes from different isolates of the same bacterial species can display considerable genetic variation³⁴, seed-transmission of these phytopathogenic microorganisms could still influence the functional composition. We therefore evaluated the impact of seed transmission of plant pathogens on the functional profile of the seed microbiome.

A total of 682,374 coding sequences (CDSs) shared in 17,589 orthologous groups (OGs) were predicted across the different metagenomic samples. On average, each metagenomic sample was composed of 8,828 OGs

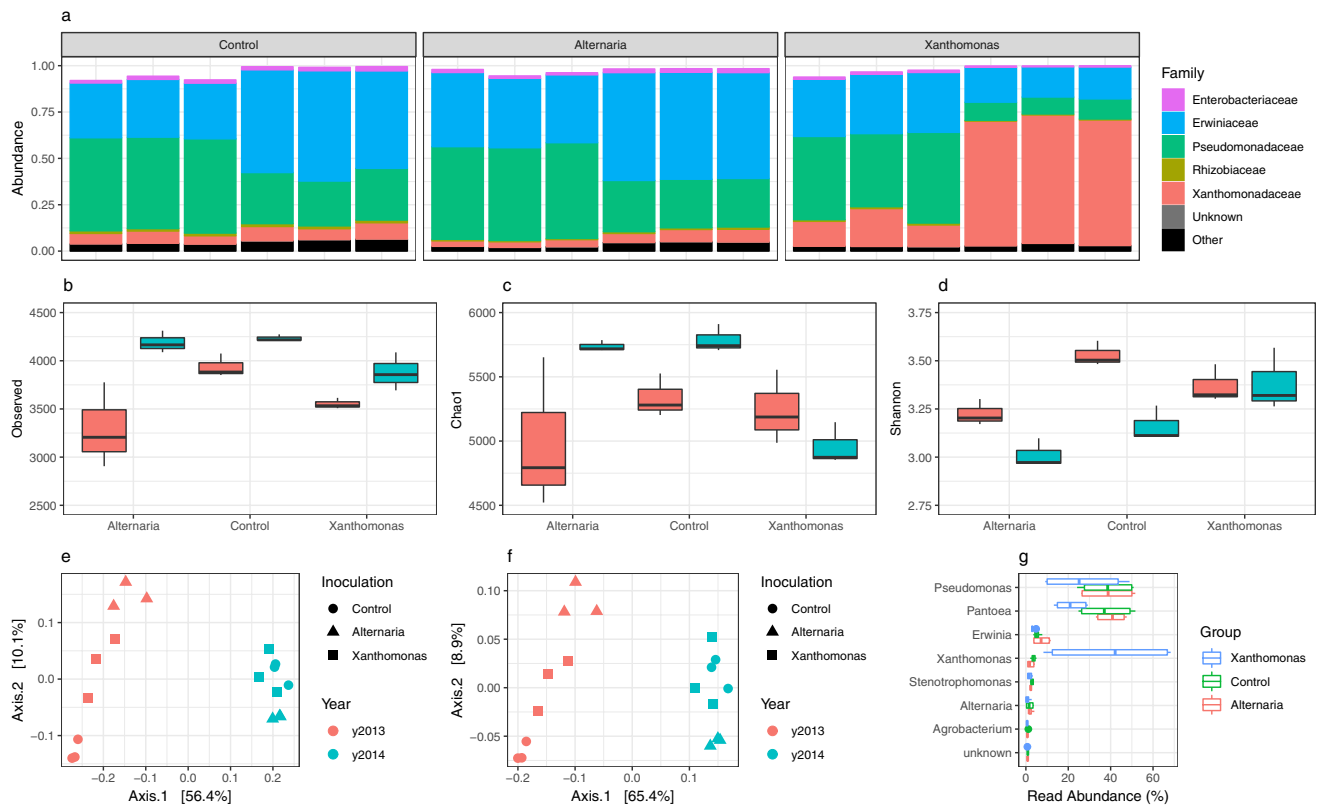


Figure 1. Changes in seed microbiome structure following seed transmission of Abra43 and Xcc8004. ParaKraken prediction of the taxonomic composition of the bacterial fraction of the radish seed microbiome (a). Measure of microbial alpha diversity through observed richness (number of predicted species), estimated richness (Chao1 index) and diversity (Shannon index) (b–d). Similarity in community membership (Jaccard index) (e) and community composition (Bray-Curtis index) (f) between seed samples. Changes in relative abundance of the 10 most abundant microbial genera following seed transmission of phytopathogenic agents (g).

(SD + 494, Fig. 2a). Seed transmission of Abra43 and Xcc8004 did not significantly alter ($P > 0.01$) the observed functional richness, the estimated functional richness and the functional diversity of the seed microbiome (Fig. 2a–c). While harvesting year significantly impacted functional membership ($P < 0.0001$, 44.4%) and functional composition ($P < 0.0001$, 52.6%) of the seed microbiome, no significant differences ($P > 0.001$) in functional membership or composition (Fig. 2d,e) were observed after seed transmission of Abra43 and Xcc8004. In addition, we did not detect any significant difference in RA of broad functional categories following pathogen transmission (Fig. 2f). Altogether these results highlight that seed transmission of Xcc8004 and Abra43 do not modify either the predicted structure or function of the seed microbiome.

While broad functional changes were not observed with seed transmission, OG RAs clustered together based upon relative shifts within the microbiome. Markov cluster algorithm of DUO networks resulted in 16 clusters (>2 OGs) with positive associations and 6 clusters with negative associations (Additional file 5). One such positive cluster is suggestive of invasion/pathogenesis of eukaryotic cells and eukaryotic cell response (Additional file 5), denoting important host and pathogen domains in response to infection.

Visualization of *Xanthomonas* spp. within seed tissues. The absence of shift in structure and function of the seed microbiome following the plant-pathogen transmission suggests that the targeted plant pathogens and the other members of the seed microbiome do not compete for nutrient and space. We first investigated the spatial localization of Xcc8004 within seeds using fluorescence *in situ* hybridization. Using surface sterilized seeds, *Xanthomonas* spp. were detected inside inoculated seeds (Fig. 3). They were particularly present in embryonic tissues, especially at the surface of the radicle among other bacteria (Fig. 3a). They were also detected, however, in other embryonic zones of the seeds. *Xanthomonas* spp. were identified in the same tissues in control samples, but with lower abundance than Xcc8004-seeds (Fig. 3b). Using a photon detection method or analog integration on confocal microscope, similar results were obtained but with brighter signals from the specific probe using analog integration (Fig. 3c,d). Interestingly, cells were single or as packs of several bacteria (Fig. 3a–d). In control and Xcc8004-inoculated seeds hybridized with negative probe, no signal was identified (Fig. 3e,f). On the internal side of the seed coat, *Xanthomonas* spp. were further identified in Xcc8004 inoculated seeds, showing different niches of colonization (Fig. 3g,h).

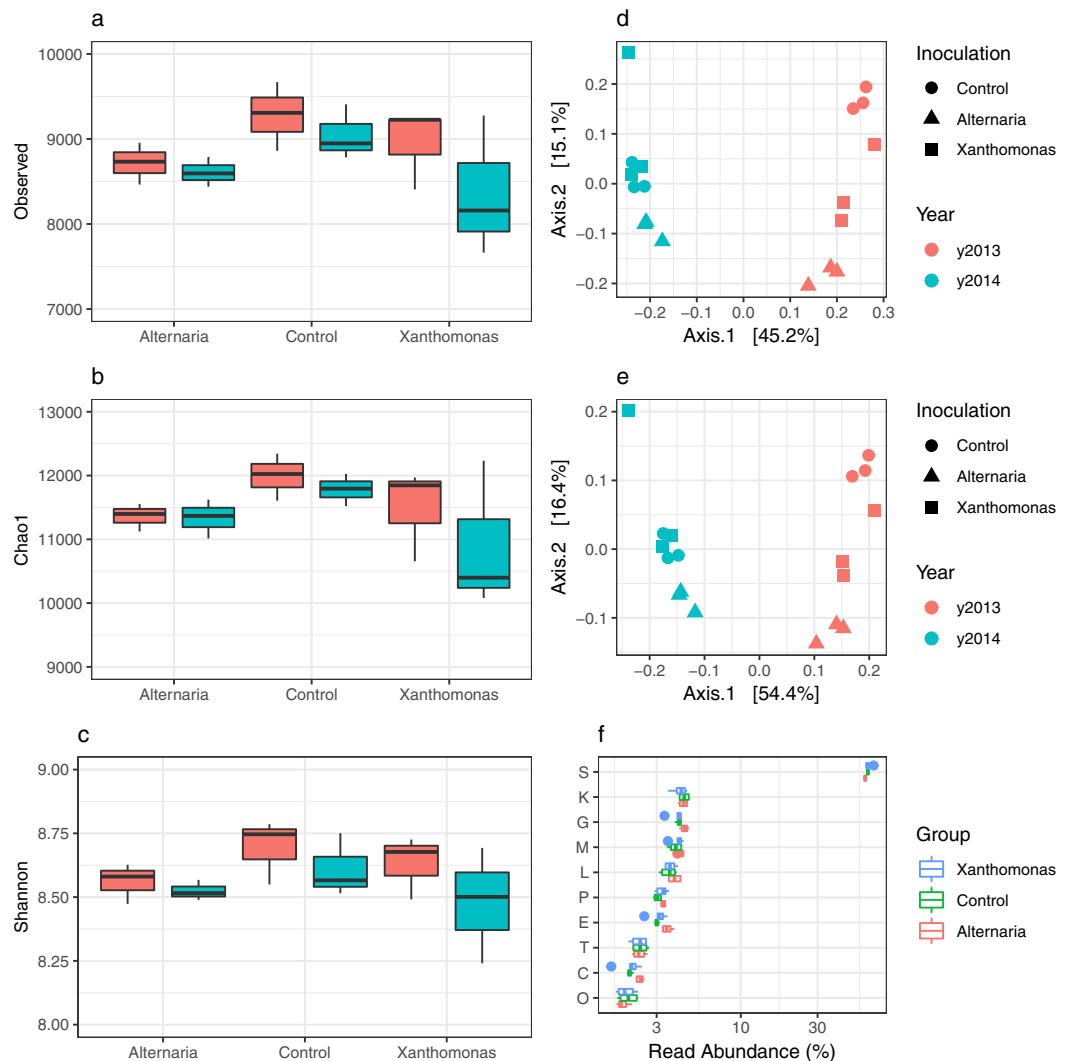


Figure 2. Changes in the functional composition of the seed microbiome following seed transmission of Abra43 and Xcc8004. Measure of observed functional richness (number of OG), estimated functional richness (Chao1 index) and functional diversity (Shannon index) (a–c). Similarity in functional membership (d) and composition (e) as assessed with Jaccard and Bray-Curtis indexes. Changes in relative abundance of broad functional categories (f).

Reconstruction of genomic sequences from the main bacterial population of the seed microbiome. Competition for nutritional resources between phytopathogenic agents and other members of the seed microbiome was subsequently estimated with genomic sequences. Given the limited number of fungal reads in our metagenomics datasets, we restricted this comparative genomic analysis to bacterial populations and Xcc8004. Bacterial genomic sequences were either recovered through metagenomic read sets or *via* genome sequencing of representative bacterial isolates (see materials and methods). Overall, 11 metagenome-assembled genomes (MAGs; >50% completeness, <10% contamination) and 21 genomes sequences were obtained (Table 1). These genomic sequences represented the major bacterial species detected with the ParaKraken taxonomic classification approach, and, based on their *gyrB* sequences, represented the main *gyrB* amplicon sequences variants (ASVs) of the radish seed microbiomes (Table 1 and Additional file 6^{24,35}). According to the average nucleotide identity based on blast (ANIb) values, these 32 genomic sequences were divided into 22 bacterial species (Additional file 7). The relative abundance of each genome sequence within the seed microbiome was estimated by mapping the metagenomics reads to these sequences and expressed as average coverage. Overall, genomic sequences related to *Pantoea agglomerans* and *Pseudomonas viridiflava* were highly abundant in all radish seed samples, with an average coverage of approximately 200X and 80X, respectively (Table 1 and Additional file 8).

Assessment of resources overlap among bacterial members of the seed microbiome. Overlap in nutritional resource use between Xcc8004 and bacterial populations from the seed microbiome was assessed by profiling nutrient consumption patterns of Xcc8004 and seed bacterial isolates with GEN III MicroPlate. Overall, the bacterial consumption pattern was largely grouped by the phylogenetic relationships between strains

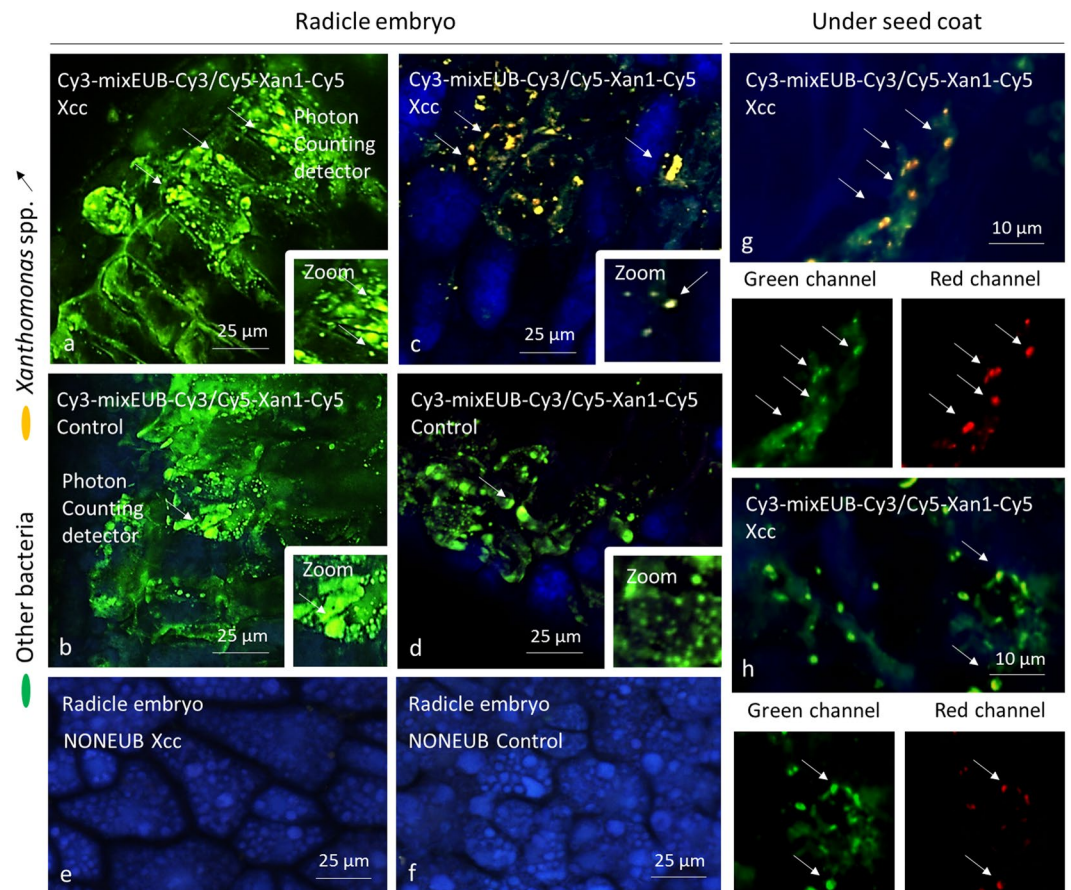


Figure 3. Visualization of *Xanthomonas* spp. inside seeds. Photon counting detection of *Xanthomonas* spp. on the radicle of the embryo following seed transmission of Xcc8004 (a) or control seeds (b). Analog integration detection of *Xanthomonas* spp. on radicle of seeds contaminated with Xcc8004 (c) or not contaminated (d). Use of NONEUB probes on samples subjected to Xcc8004 (e) or control seeds (f). Detection of *Xanthomonas* spp. under the seed coat (g,h). Bacteria corresponding to *Xanthomonas* spp. appear as yellow/orange fluorescents after blue, green and red channels were merged or as red if channels are separated while other bacteria appear as green fluorescents.

(Additional file 9). Overlap in nutritional resources between Xcc8004 and seed-associated bacterial strains ranged from 0.23 to 0.50, with the highest overlap being observed with strains CFBP13503 and CFBP13529 of *Stenotrophomonas rhizophila* (Fig. 4).

Since the compounds reduced in GEN III MicroPlates by the bacterial strains are neither representative of all seed exudates compounds nor a reflection of their actual concentrations³⁶, we further assessed similarities/differences in nutritional resources consumption between Xcc8004 and the other bacterial members of the seed microbiome by using MAGs and draft genome sequences and genome sequences. We compared the number of predicted OGs associated with amino acid [E], carbohydrate [G], lipid [I] and inorganic ion [P] transport and metabolism (Fig. 4). The highest median overlap was observed with the functional categories E (0.61) and I (0.66), while the median overlap for G and P was below 0.5. In all cases, the most pronounced resource overlap was associated with genome sequences of *Xanthomonadales* (Fig. 4).

To determine if the observed resource overlap was associated with a decrease of Xcc8004 population during competition with these bacterial strains, co-inoculation of Xcc8004 was performed with each seed bacterial isolate on radish seed exudates media (see Materials and Methods). We observed a significant decrease ($P < 0.01$) in Xcc8004 CFU at 2, 3, 4 and 5 dpi during co-inoculation with strains CFBP13503 and CFBP13529 (Fig. 5). This effect seems to be dependent on competition for nutritional resources, since no direct antagonism was observed between Xcc8004 and *S. rhizophila* strains during overlay assay (data not shown). To gain insight into potential competition for nutrients between Xcc8004 and *S. rhizophila* strains, we compared the set of OGs that were exclusively shared between these strains (Additional file 10). A total of 251 CDSs divided into 219 OGs were specifically shared between Xcc8004 and *S. rhizophila*. While, most of these OGs have no predicted function, nine CDSs were related to carbohydrate utilization (pectate lyase, mannosidase and glucosidase). In addition, multiple protein-coding genes involved in rapid utilization of the limiting resource(s), such as TonB-dependent transporters (TBDTs) were also shared between the *Xanthomonadales* strains (Additional file 10).

Genome	Plot	<i>gyrB</i> ASV	ASV frequency (330 samples)	Size (nucleotides)	Number of contig	Number of predicted CDS	Number of OG	Average coverage	ANiB	Closest genome (ANiB)
bin01	NA	ASV00004	98.5	4,912,500	59	4,833	4,466	16.2	0.99	<i>Erwinia persicina</i> NBRC 102418
bin05	NA	NA	NA	4,747,556	264	4,770	4,327	4.7	0.98	<i>Pseudomonas</i> sp. 1R 17
bin06	NA	ASV00021	33.8	6,545,609	154	8,432	7,592	8.4	0.97	<i>Pseudomonas moraviensis</i> R28-S
bin09	NA	ASV00006	67.1	6,155,276	68	6,873	6,141	45.0	0.97	<i>Pseudomonas viridiflava</i> LMCA8
bin11	NA	ASV00299	7.9	4,444,399	576	3,772	3,498	2.8	0.98	<i>Paenibacillus</i> sp. TI45-13ar
bin13	NA	ASV00224	15.7	4,861,286	176	4,374	3,799	3.0	0.98	<i>Stenotrophomonas maltophilia</i> PierC1
bin22	NA	ASV01700	3.3	3,596,431	121	3,329	2,848	4.4	0.96	<i>Chryseobacterium indeothelicum</i> DSM 16778
bin23	NA	ASV00037	31.1	5,194,700	5	4,419	3,922	66.1	1.00	<i>Xanthomonas campestris</i> pv. <i>campestris</i> 8004
bin25	NA	NA	NA	4,053,393	156	3,631	3,319	1.2	0.94	<i>Pseudomonas thivervalensis</i> B3779
bin27	NA	ASV00001	100	4,120,090	33	4,886	4,644	171.0	0.98	<i>Pantoea agglomerans</i> NBRC 102470
bin31	NA	ASV00288	11.8	2,686,338	295	2,607	2,411	0.7	0.98	<i>Enterobacter cloacae</i> EcWSU1
CFBP 13502	C2013	ASV00008	25.7	6,144,992	53	5,570	5,079	17.3	0.99	<i>Pseudomonas fluorescens</i> WH6
CFBP 13503	X2013	ASV00027	65.9	4,855,517	35	4,275	3,693	10.4	0.96	<i>Stenotrophomonas rhizophila</i> DSM 14405
CFBP 13504	A2013	ASV00041	16.6	6,595,509	85	5,842	5,228	18.4	0.97	<i>Pseudomonas koreensis</i> CI12
CFBP 13505	X2014	ASV00001	100	4,863,834	48	4,490	4,204	204.5	0.98	<i>Pantoea agglomerans</i> LMAE-2
CFBP 13506	X2014	ASV00014	39.3	5,914,838	43	5,356	4,937	18.1	1.00	<i>Pseudomonas</i> sp. 31 E 5
CFBP 13507	X2014	ASV00002	100	5,881,917	51	5,206	4,715	81.6	0.97	<i>Pseudomonas viridiflava</i> LMCA8
CFBP 13508	C2014	ASV00031	20.5	6,000,531	26	5,258	4,762	28.5	0.95	<i>Pseudomonas</i> sp. R62
CFBP 13509	C2014	ASV00011	61.3	6,792,256	58	6,082	5,605	20.7	0.99	<i>Pseudomonas</i> sp. 8R 14
CFBP 13510	C2014	ASV00139	10.3	6,347,968	55	5,628	5,101	20.5	0.99	<i>Pseudomonas fluorescens</i> SS101
CFBP 13511	X2014	ASV00004	98.5	5,203,109	112	4,853	4,503	9.8	0.99	<i>Erwinia persicina</i> NBRC 102418
CFBP 13512	X2014	ASV00170	16.0	5,211,788	49	4,612	4,024	4.2	0.98	<i>Paenibacillus</i> sp. TI45-13ar
CFBP 13513	C2014	ASV00136	75.5	4,231,965	7	3,897	3,452	0.7	0.95	<i>Plantibacter flavus</i> 251
CFBP 13514	C2014	ASV00057	39.3	6,238,853	29	5,618	5,151	16.0	0.99	<i>Pseudomonas fluorescens</i> PICE7
CFBP 13515	X2014	ASV00002	100	5,869,336	150	5,212	4,709	82.2	0.97	<i>Pseudomonas viridiflava</i> LMCA8
CFBP 13516	X2014	ASV00001	100	5,026,237	54	4,676	4,329	200.1	0.98	<i>Pantoea agglomerans</i> LMAE-2
CFBP 13517	C2014	ASV00010	35.6	5,954,142	63	5,365	4,873	19.1	0.99	<i>Pseudomonas fluorescens</i> PT14
CFBP 13528	X2014	ASV00009	49.2	5,999,230	44	5,298	4,765	17.1	0.99	<i>Pseudomonas</i> sp. 37R 15
CFBP 13529	X2014	ASV00027	65.9	4,626,295	12	3,990	3,505	11.0	0.96	<i>Stenotrophomonas rhizophila</i> DSM 14405
CFBP 13530	C2013	ASV00076	25.7	4,901,530	37	4,563	4,371	3.0	0.99	<i>Enterobacter cancerogenus</i> ATCC 35316
CFBP 13532	X2013	ASV00001	100	4,934,344	61	4,599	4,277	202.5	0.98	<i>Pantoea agglomerans</i> LMAE-2
Xcc1	NA	ASV00037	31.1	5,169,428	1	4,372	3,886	80.7	1.00	<i>Xanthomonas campestris</i> pv. <i>campestris</i> 8004
Xcc2	X2014	ASV00037	31.1	5,161,175	1	4,354	3,872	81.3	1.00	<i>Xanthomonas campestris</i> pv. <i>campestris</i> 8004

Table 1. Characteristics of the genomes sequences reconstructed from metagenomic reads or sequencing of some bacterial isolates. The experimental plot from where the bacterial isolate was obtained, *gyrB* amplicons sequence variant (ASV), genome size, number of contigs, number of predicted CDS, number of orthologous groups (OG), average genome coverage, average nucleotide identity based on blast (ANiB), closest genomes sequence based on ANiB are indicate.

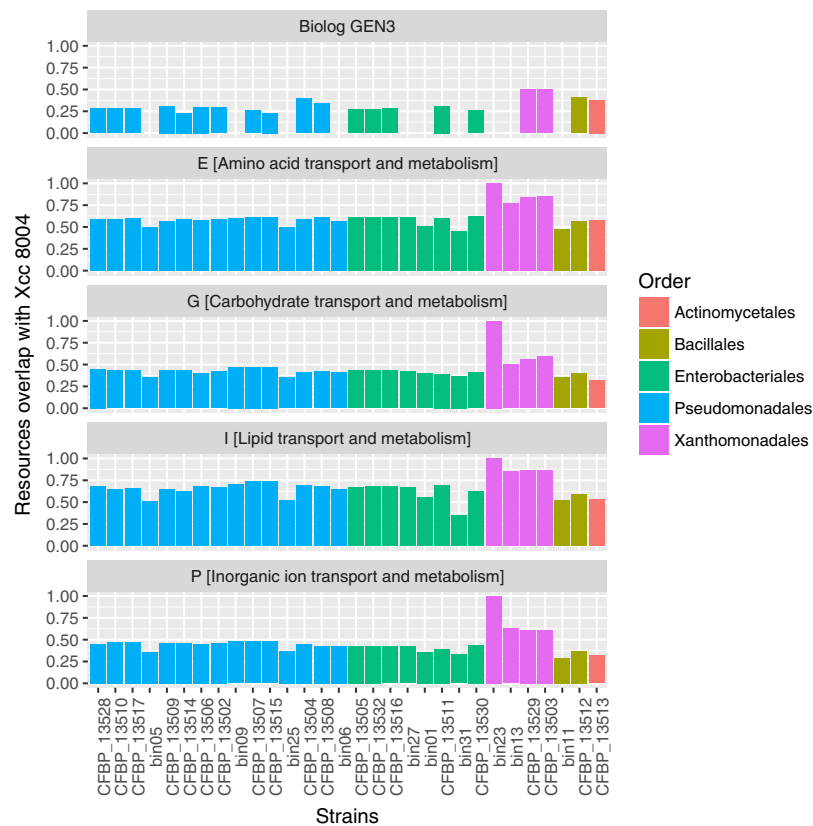


Figure 4. Resources overlap between Xcc8004 and bacterial populations of the seed microbiome. Resource consumption pattern was either assessed with Biolog GEN III MicroPlate or with orthologous groups (OGs) predicted from bin/genomic sequences. Resources overlap was defined as the number of shared resources between Xcc8004 and the tested bacterial strain, divided by the total number of resources used by Xcc8004 and the tested strain.

Dynamics of seed-associated microbial taxa during plant germination and emergence. Microbial populations associated with seeds could be either transient colonizers (i.e. seed-borne) or transmitted during germination and emergence to the seedling (seed-transmitted). To investigate which bacterial populations associated with radish seed samples contaminated with Xcc8004 were seed-transmitted, we performed community profiling with *gyrB* on germinating seeds and seedlings. According to the number of *gyrB* sequences detected during these early stages of the plant life's cycle, ASVs belonging to the bacterial species *P. agglomerans*, *P. viridiflava* and species of the *P. fluorescens* group were efficiently transmitted to seedlings (Additional file 11). Moreover, ASVs belonging to Xcc8004 and *S. rhizophila* were also detected in germinating seeds and radish seedlings (Additional file 11). The competition for resources between Xcc8004 and *S. rhizophila* strains observed on exudates media (Fig. 5) and the co-occurrence of these two species within germinating seeds and seedlings either suggest that resources are not a limiting factor within these habitats or that both species are located in different tissues.

Discussion

Microbial interactions occurring on and around the seed are important for plant fitness, since seed-borne microorganisms are the primary source of inoculum for the plant. Depending on the outcome of the interactions, these microbial assemblages could either promote or reduce plant growth⁹. Understanding the processes involved in the assembly and resilience of the seed microbiota is especially relevant to comprehend the emergence of plant diseases. In the current work we assessed whether niche preemption occurred during seed-transmission of two phytopathogenic agents, Xcc8004 and Abra43, which differ in their transmission modes.

According to our metagenomic datasets, the radish seed microbiome was mostly composed of eubacteria. Whether this estimation reflects the actual structure of the radish seed microbiome or represents a bias due to DNA extraction/classification methods is currently unknown. Bacterial communities of radish seeds were dominated by two bacterial families, the *Erwiniaceae* and *Pseudomonadaceae*. More precisely, bacterial populations affiliated with *Pantoea agglomerans*, *Erwinia persicina*, *Pseudomonas viridiflava*, *P. fluorescens* and *P. koreensis* groups were associated with all radish seed samples. These species have been frequently reported in seeds of Brassicaceae^{24,35,37–39} and in other plant families such as Fabaceae³⁷, Amaranthaceae³⁸ or Poaceae^{39,40}. The high prevalence of these taxa in various seed samples may be explained by specific determinants that could help these microorganisms to thrive in the seed habitat. For instance, seed-transmitted microorganisms should deal with the high level of basal defense response related to reproductive organs^{41–43} and tolerate desiccation occurring during seed maturation⁴⁴. In addition, the high abundance and occurrence of these bacterial populations within seed

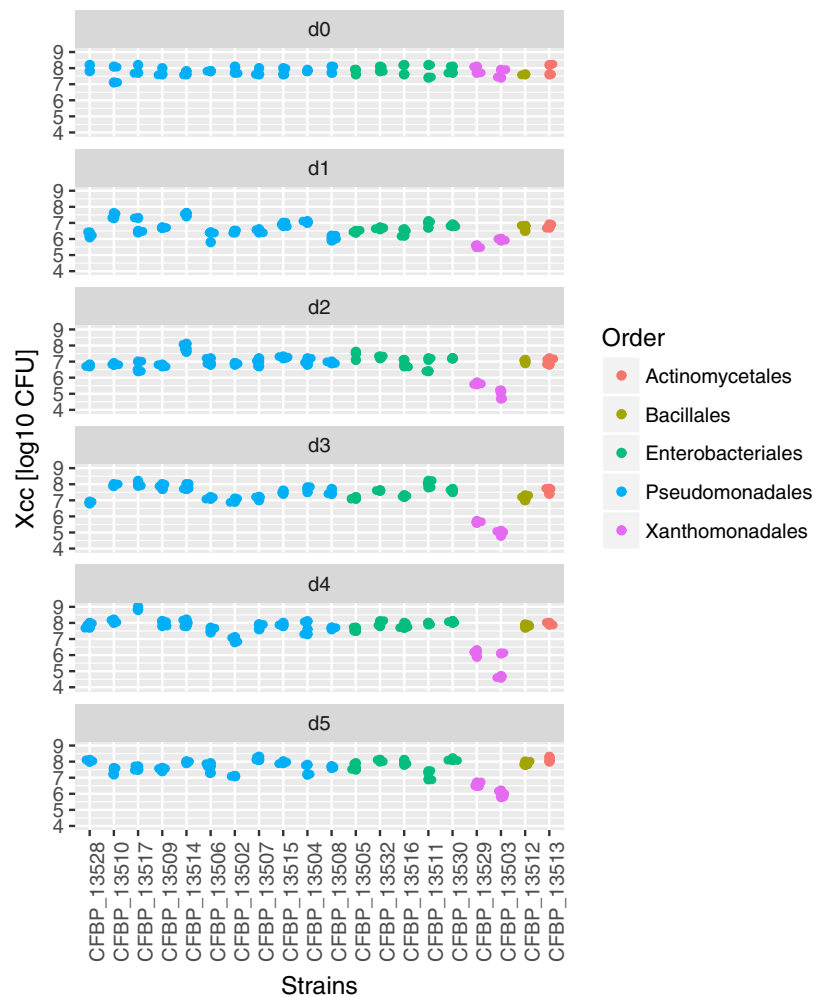


Figure 5. Competition for resources between Xcc8004 and bacterial populations of the seed microbiome. Competition between Xcc8004 and seed bacterial isolates was performed at a 1:1 ratio on radish exudates media. Bacterial spots were removed 1, 2, 3, 4 and 5 days post-inoculation and the number of colony forming units of Xcc8004 (y-axis) was recorded on TSA10% supplemented with rifampicin and X-Gluc. Three independent biological replicates, each consisting of 3 technical replicates, were performed. Differences in number of CFUs per treatment were assessed by one-way ANOVA with post-hoc Tukey's HSD test.

samples suggested that these taxa could influence the community structure of the plant microbiome during its early developmental stages. This assumption remained to be validated experimentally through synthetic ecology approaches as recently performed in the maize rhizosphere⁴⁵.

In our experimental design, the impact of Xcc8004 and Abra43 transmission on the structure and function of the seed microbiome was assessed during two consecutive years. The changes in taxonomic and functional profiles were mostly driven by the harvesting year, thus confirming previous results obtained through community profiling approaches^{35,37,46}. This is perhaps not surprising, as abiotic factors, such as soil or field management practices, have been already observed to have a strong influence in the seed microbiota³⁷. In contrast, the seed transmission of the two plant pathogens, Xcc8004 and Abra43, did not impact the overall composition of the seed microbiome.

Previous reports have shown that Xcc8004 is seed-transmitted through the xylem and the stigma, while Abra43 is seed-transmitted *via* fruits^{30–32}. Hence Xcc8004 is probably one of the primary colonists of the seed microbiota, while Abra43 is a late-arriving species. Although both phytopathogenic agents were efficiently transmitted to radish seeds, they impacted neither the structure nor the function of the seed microbiome, implying that they are not competing with the other members of the microbiome for the same ecological niches in the seed habitat. According to *in situ* hybridization, *Xanthomonas* sp. co-occurred with other bacterial taxa within the seed coat and at the surface of the seed embryo. Since no spatial separation was observed between Xcc8004 and other seed-borne bacterial populations, then differences in resources consumption can probably explain this co-existence. Based on our genomics prediction of resource overlap and competition assays performed on radish exudate media, most of the bacterial populations of the seed microbiome are not competing with Xcc8004 for nutritional resources. Although the competition assay performed does not necessary reflect the actual

composition and concentration of nutrients that are available for microbial growth during seed development^{36,47}, it can serve as a proxy for assessing competition between seed-borne bacterial species.

Under our experimental conditions, the only bacterial population that competes for nutritional resources with Xcc8004 belongs to the species *S. rhizophila*. Competition for a limiting resource can be divided into two categories: exploitative competition that is related to the rapid use of the limiting resource and contest competition that involves antagonistic interactions with production of antimicrobial compounds⁴⁸. As we did not observe an antagonistic relationship with the overlay assay used in this work, the observed competition between *S. rhizophila* strains and Xcc8004 is likely due to resources use⁴⁹. This contest competition is frequently related to efficient uptake of nutrients by the competing species⁴⁸. Interestingly numerous OGs that are specifically shared between Xcc8004 and *S. rhizophila* strains CFBP13503 and CFBP13529 are related to TBDTs, which form a specific carbohydrate utilization system⁵⁰.

According to the community profiling approach performed on more than 300 radish seed samples^{24,35}, it appears that *S. rhizophila* strains and Xcc8004 co-exist within the seed habitat. Moreover, both bacterial species co-occurred on germinating seeds and seedlings during germination and emergence, suggesting that nutritional resources are not limited enough within these habitats for observing a strong niche preemption. Alternatively, we cannot rule out the hypothesis of both species being not spatially related. In contrast to Xcc8004, *S. rhizophila* is mainly located at the seed surface of radish, since no strains were recovered after seed surface sterilization (unpublished observations). Seed surface localization is in accordance with the epiphytic localization of *S. rhizophila* DSM 14405 on leaves and roots tissues of cotton, sweet pepper and tomato⁵¹. Owing to this predicted localization, it is tempting to postulate that *S. rhizophila* is a late colonist of the seed microbiome, being transmitted through the external pathway.

Nowadays, sanitary quality of seeds is achieved through chemical methods and prophylaxis measures. Since reducing pesticide usage is an important objective for sustainable agriculture, the search for alternative seed treatments is essential. One of these alternative treatments consists in coating the seeds with microorganisms possessing biocontrol activities. However, biocontrol-based strategies require a better understanding of the colonization abilities of the microbial consortia within the seed habitat and its persistence within the spermosphere²¹. Our data showed that *S. rhizophila* and Xcc8004 have a high resource overlap and can compete *in vitro* for resources. An interesting approach to restrict seed transmission of Xcc8004 could be the introduction of *S. rhizophila* into the seed tissues with EndoSeed™ technology²⁰. Inoculation would encourage the co-existence of both taxa within the same ecological niche and maybe limit the size of Xcc8004 population within seed tissues. In addition to this augmentative biological control strategy, the limitation of Xcc8004 transmission could be potentially obtained by sowing radish seeds in plots containing a high-level of *S. rhizophila*. Indeed, the composition of the spermosphere-associated microbial assemblages is highly influenced by local horizontal transmission⁵². All things considered, *S. rhizophila* seems to be a promising candidate to reduce seed transmission of the pathogen Xcc8004, although further seed transmission experiments are needed to corroborate the fate of these taxa *in planta*. Collectively, these data may serve as a foundation for further research towards the design of novel biocontrol-based strategies on seed samples.

Conclusions

Seed-transmission of phytopathogenic agents is significant for disease emergence and spread. In the present study, we have shown that the presence of Abra43 and Xcc8004 within radish seed samples did not modify the structure and function of the seed microbiome. The absence of community shift is explained in part by the low overlap in the use of resources between Xcc8004 and the main seed-borne bacterial populations. However, we have identified potential competitors of Xcc8004 belonging to *S. rhizophila* species. Understanding the pathways and determinants of seed transmission of Xcc8004 and *S. rhizophila* can result in the subsequent design of efficient management methods for restricting prevalence of phytopathogenic agents within seed samples through niche preemption²¹. More generally, the metagenomic sequences obtained in this work provide a starting point to investigate the genomic features involved in seed transmission through comparative genomics with bacterial isolates recovered from other plant habitats such as the rhizosphere or the phyllosphere⁵³. Our approach of coupling community profiling approaches, bacterial confrontational assays and fluorescent *in situ* hybridization methods opens the way for further target research on seed inoculations with microorganisms possessing plant-beneficial properties.

Materials and Methods

Seed collection, DNA extraction and shotgun metagenomic libraries preparation. The seed samples used in this work were collected in 2013 and 2014 during experiments thoroughly described elsewhere²⁴. Briefly, radish seeds (*Raphanus sativus* var. Flamboyant5) were harvested at the FNAMS experimental station (47°28'12.42"N, 0°23'44.30"W, Brain-sur-l'Authion, France). These seed samples were collected from plants inoculated with *Alternaria brassicicola* strain Abra43; plants inoculated with *Xanthomonas campestris* pv. *campestris* strain 8004 and control plants without pathogen inoculation. To assess variation in seed community composition, every seed sample (A2013, A2014, C2013, C2014, X2013 and X2014) was divided into 3 subsamples (pseudo-replicates) of 10,000 seeds, resulting in a total of 18 samples (Additional file 1). In addition, a fourth subsample of 10,000 seeds was collected from the X2013 sample for PacBio sequencing.

DNA extraction was performed on seed samples according to the procedure described earlier⁴⁶ (see Text S1 in the Supplementary material for protocol details). DNA samples were sequenced at the Genome-Transcriptome core facilities (Genotoul GeT-PlaGe; France). Illumina sequencing libraries were prepared according to Illumina's protocols using the Illumina TruSeq Nano DNA LT Library Prep Kit. DNA-sequencing experiments were performed on an Illumina HiSeq3000 using a paired-end read length of 2 × 150 bases with the Illumina HiSeq3000 Reagent Kit. Each library was sequenced on three lanes of HiSeq3000. PacBio sequencing was performed on a

RSII system (details in Text S1). PacBio reads were used to improve the contigs length of the meta-assembly but were not used to assess differences in taxonomic/functional compositions. 0.25 nM of libraries were loaded per SMRTcell on the PacBio RSII System and sequencing was performed on 6 SMRTcells using the OneCellPerWell Protocol (OCPW) on C4P6 chemistry and 360 minutes movies.

Metagenomic read processing. Sequencing of the 18 metagenomic seed samples resulted in a mean of 15.3 million paired-end reads per sample (SD + 3.3 million). These paired-end reads were processed with cutadapt version 1.8⁵⁴ to remove Illumina's adapters, bases with Qscore < 25, reads possessing more than one ambiguity and paired-end reads with a length < 100 bases. Host-related reads were removed with Bowtie2 version 2.2.4⁵⁵. Quality filtering of raw reads resulted in a mean of 12.5 million paired-end reads (SD + 2.7 million) per metagenomics read set, which corresponds to approximately 2.5 Gb per metagenome (Text S1 and Additional file 1).

Taxonomic inference of metagenomics reads. The relative abundances of Xcc8004 and Abra43 within seed samples were estimated by mapping metagenomic reads to their respective genome sequences^{23,56}. Taxonomic profiling of each metagenome was estimated with a modified parallel version of Kraken⁵⁷, named ParaKraken³³, creating a count table of species and a relative abundance for each sample. Reads affiliated with the species *Xanthomonas campestris* and *Alternaria brassicicola* were removed in the count table for richness and diversity analyses (see Text S1 for details).

Richness and diversity were calculated with the R package phyloseq 1.22.3⁵⁸ on species count table. Differences in observed richness, estimated richness and diversity between samples were assessed through Kruskal-Wallis non parametric analysis of variance followed by Dunn's post-hoc test. Differences in community membership and composition were estimated with the Jaccard and Bray-Curtis index. Principal coordinate analysis (PCoA) was used for ordination of Jaccard and Bray-Curtis distances. A permutational multivariate analysis of variance (PERMANOVA) was carried out to assess the impact of pathogen transmission on seed-associated microbial community profiles. To quantify the contribution of the seed transmission of phytopathogenic microorganisms on microbial community profiles, a canonical analysis of principal coordinates (CAP) was performed with the function capscale of the R package vegan 2.4.2, followed by PERMANOVA with the function adonis.

To investigate changes in the relative abundance between the different seed samples, rare species (those occurring in less than 75% of the samples) were first removed from the species count table. Fcros differential abundance analysis³¹ was then performed between each sample pair on all species and just the species with the highest abundance (>0.1% RA). A p-value cutoff of 0.05 and an f-score of 0.9 were used to determine differential abundance. The species scaled data was also run through DUO (<https://github.com/climers/duo.git>) with a threshold of >0.75, a program that identifies positive and negative relationships between species. Briefly, DUO first identifies abundance thresholds of 75th and 25th percentiles. The percentiles are then used to identify relationships between taxa by generating four categories (high-high, high-low, low-high, and low-low) based upon the CCC metric³².

Functional profiling of each metagenome. An assembly of Illumina and PacBio metagenomic reads was performed with IDBA_UD⁵⁹ and HGAP3⁶⁰, resulting in a non-redundant assembly of circa 1 Gb containing 317,206 contigs (Additional file 12). A gene catalogue was created through gene prediction with Prokka 1.12⁶¹. Orthology inference of the 930,134 predicted CDSs was performed with DIAMOND⁶² against the EggNOG v4.5 database⁶³. Approximately 73% of the predicted CDSs (682,374 CDSs) were affiliated with one orthologous group (OG).

To avoid an overrepresentation of orthologous groups (OGs) related to the inoculated phytopathogenic agents, reads that were mapped to Xcc8004 and Abra43 genomes were discarded. The remaining metagenomic reads were mapped with BowTie2 against all predicted CDSs and converted to bam files with Samtools v1.2.1⁶⁴. Bam files were used to count the number of reads occurrence within each predicted CDS.

Similar to the species counts data, the OG counts were run through DUO with a threshold of >0.75 to identify positive (up-up and down-down) and negative (down-up and up-down) relationships between OGs to hypothesize which functional elements may interact. OG DUO networks were split into a network of positive interactions and negative interactions and then clustered using MCL⁶⁵ to identify groups of highly interconnected OGs.

Reconstruction of metagenome-assembled genomes. Initial binning was performed with Metabat v. 0.32.4⁶⁶. Metagenome-assembled genomes completeness, contamination and strain heterogeneity were evaluated with CheckM v 1.0.4⁶⁷. Taxonomic affiliation of each bin was performed by Average Nucleotide Identity based on BLAST (ANiB) with Jspecies⁶⁸. Closest ANiB values were selected for reference genomes and used for Circle Packing representation with the D3.js JavaScript library representation (see details in Text S1).

Reconstruction of genomic sequences of seed-associated bacterial isolates. Approximately 200 bacterial strains from the seed samples used for the metagenomics analysis were isolated on 1/10 strength Tryptic Soy Agar (Text S1). A total of 21 representative isolates of the main bacterial taxa were subjected to Illumina HiSeq 4000 PE150 sequencing (Table 1 and Additional File 6). These isolates were chosen by comparing their *gyrB* haplotypes with *gyrB* sequences previously obtained on radish seed samples²⁴. All genome sequences were assembled with SOAPdenovo 2.04⁶⁹ and VELVET 1.2.10⁷⁰, annotated with prokka⁶¹ and EggNOG 4.5⁶³.

Characterization of resource overlap between seed-associated bacterial isolates. Nutritional resource consumption patterns of bacterial strains were assessed with Biolog GEN III MicroPlate™ (Biolog Inc) (see details in Text S1 in Supplementary data). One Biolog GEN III MicroPlate™ was used per isolate. The nutritional resources overlap was also predicted by comparing the numbers of OGs that are classified in the following functional categories: [E] amino acid transport and metabolism, [G] carbohydrate transport and metabolism, [I]

lipid transport and metabolism and [P] inorganic ion transport and metabolism. Competition for resources and direct antagonisms between Xcc8004 and the selected bacterial strains were assessed on radish exudates and TSA 10% media (details in Text S1).

Community profiling of germinating seeds and radish seedlings. Seed samples harvested in plot X2014 were used to determine the dynamics of bacterial population during germination and emergence of radish. DNA extraction and subsequent *gyrB* amplicon library preparation were performed on germinating seed ($n = 6$) and seedling ($n = 8$) samples according to the procedure described earlier⁴⁶ (see details in Text S1). Libraries were sequenced with a MiSeq reagent kit v2 (500 cycles). Fastq files were processed with DADA2 1.6⁷¹ using the parameters described in the workflow for “Big Data: Paired-end”. The only modification made regarding this protocol was a change in the truncLen argument according to the quality of the sequencing run. Species abundance was assessed on germinating seed and seedling samples with the R package phyloseq⁵⁸ (ASVs taxonomic affiliation details in Text S1).

DOPE-FISH and CLSM microscopy of Xcc8004 infected seeds. Seeds were surface-sterilized, cut in half and fixed in a paraformaldehyde solution. DOPE-FISH was performed with probes from Eurofins (Austria) labeled at both the 5' and 3' end positions according to Glassner *et al.*⁷² using an EUBmix targeting all bacteria (EUB338, EUB338II, EUB338III) coupled with the fluorochrome Cy3^{73,74}, and a *Xanthomonas* spp. targeting probe (5'-TCATTCAATCGCGCGAAGCCCG-3') coupled with Cy5⁷⁵. A NONEUB probe⁷⁶ coupled with Cy3 or Cy5 was also used independently as a negative control (further protocol details in Text S1). Samples were observed under a confocal microscope (Olympus Fluoview FV1000 with multiline laser FV5-LAMAR-2 HeNe(G) and laser FV10-LAHEG230-2) (see Text S1 for image processing details). Pictures were cropped, and whole pictures were sharpened to better observe the image details. All experiments were repeated on eight seeds for each condition. Images presented in this publication are the average of colonization.

Data Availability

The datasets supporting the conclusions of this article are available in the SRA database under the accession number PRJNA454584. Whole Genome Shotgun projects have been deposited at GenBank under the accessions QFZV00000000-QGAM00000000. All bacterial strains have been deposited at the CIRM-CFBP (https://www6.inra.fr/cirm_eng/CFBP-Plant-Associated-Bacteria; <https://doi.org/10.15454/1.5103266699001077E12>).

References

- Panke-Buisse, K., Poole, A. C., Goodrich, J. K., Ley, R. E. & Kao-Kniffin, J. Selection on soil microbiomes reveals reproducible impacts on plant function. *The ISME Journal* **9**, 980–9 (2015).
- Lau, J. A. & Lennon, J. T. Rapid responses of soil microorganisms improve plant fitness in novel environments. *Proc. Natl. Acad. Sci. USA* **109**, 14058–62 (2012).
- Mendes, R. *et al.* Deciphering the rhizosphere microbiome for disease-suppressive bacteria. *Science* **332**, 1097–100 (2011).
- Sugiyama, A., Bakker, M. G., Badri, D. V., Manter, D. K. & Vivanco, J. M. Relationships between Arabidopsis genotype-specific biomass accumulation and associated soil microbial communities. *Botany* **91**, 123–126 (2013).
- Bulgarelli, D. *et al.* Revealing structure and assembly cues for Arabidopsis root-inhabiting bacterial microbiota. *Nature* **488**, 91–95 (2012).
- Maignien, L., DeForce, E. A., Chafee, M. E., Eren, A. M. & Simmons, S. L. Ecological Succession and Stochastic Variation in the Assembly of Arabidopsis thaliana Phyllosphere Communities. *mBio* **5**, (2014).
- Edwards, J. *et al.* Structure, variation, and assembly of the root-associated microbiomes of rice. *Proc. Natl. Acad. Sci. USA* **112**, E911–E920 (2015).
- Leff, J. W., Lynch, R. C., Kane, N. C. & Fierer, N. Plant domestication and the assembly of bacterial and fungal communities associated with strains of the common sunflower, *Helianthus annuus*. *New Phytol.* **214**, 412–423 (2017).
- Shade, A., Jacques, M.-A. & Barret, M. Ecological patterns of seed microbiome diversity, transmission, and assembly. *Curr. Opin. Microbiol.* **37**, 15–22 (2017).
- Rodrigues Pereira, A. S., Houwen, P. J. W., Deurenberg-Vos, H. W. J. & Pey, E. B. F. Cytokinin and the bacterial symbiosis of *Ardisia* species. *Zeitschrift für Pflanzenphysiologie* **68**, 170–177 (1972).
- Goggin, D. E., Emery, R. J., Kurepin, L. V. & Powles, S. B. A potential role for endogenous microflora in dormancy release, cytokinin metabolism and the response to fluridone in *Lolium rigidum* seeds. *Annals of botany* **115**, 293–301 (2015).
- Vázquez-de-Aldana, B. R., García-Ciudad, A., García-Criado, B., Vicente-Tavera, S. & Zabalgoitia, I. Fungal Endophyte (*Epichloë festucae*) Alters the Nutrient Content of *Festuca rubra* Regardless of Water Availability. *PLOS ONE* **8**, e84539 (2013).
- Baker, K. F. & Smith, S. H. Dynamics of Seed Transmission of Plant Pathogens. *Annual Review of Phytopathology* **4**, 311–332 (1966).
- Gitaitis, R. & Walcott, R. The epidemiology and management of seedborne bacterial diseases. *Annual Review of Phytopathology* **45**, 371–97 (2007).
- Darrasse, A., Bureau, C., Samson, R., Morris, C. & Jacques, M.-A. Contamination of bean seeds by *Xanthomonas axonopodis* pv. *phaseoli* associated with low bacterial densities in the phyllosphere under field and greenhouse conditions. *European Journal of Plant Pathology* **119**, 203–215 (2007).
- Darrasse, A. *et al.* Transmission of Plant-Pathogenic Bacteria by Nonhost Seeds without Induction of an Associated Defense Reaction at Emergence. *Applied and Environmental Microbiology* **76**, 6787–6796 (2010).
- Darsonval, A. *et al.* The Type III secretion system of *Xanthomonas fuscans* subsp. *fuscans* is involved in the phyllosphere colonization process and in transmission to seeds of susceptible beans. *Applied and Environmental Microbiology* **74**, 2669–78 (2008).
- Valeria, M. & Gianfranco, R. Seed treatments to control seedborne fungal pathogens of vegetable crops. *Pest Management Science* **70**, 860–868 (2013).
- Wightwick, A., Walters, R., Allinson, G., Reichman, S. & Menzies, N. Environmental Risks of Fungicides Used in Horticultural Production Systems. *Fungicides*, doi:10.5772/13032 (2010).
- Mitter, B. *et al.* A New Approach to Modify Plant Microbiomes and Traits by Introducing Beneficial Bacteria at Flowering into Progeny Seeds. *Front. Microbiol.* **8**, (2017).
- Barret, M., Guimbaud, J.-F., Darrasse, A. & Jacques, M.-A. Plant microbiota affects seed transmission of phytopathogenic microorganisms. *Molecular Plant Pathology* **17**, 791–795 (2016).

22. Jakuschkin, B. *et al.* Deciphering the Pathobiome: Intra- and Interkingdom Interactions Involving the Pathogen *Erysiphe alphitoides*. *Microb. Ecol.* **72**, 870–880 (2016).
23. Qian, W. *et al.* Comparative and functional genomic analyses of the pathogenicity of phytopathogen *Xanthomonas campestris* pv. *campestris*. *Genome research* **15**, 757–67 (2005).
24. Rezki, S. *et al.* Differences in stability of seed-associated microbial assemblages in response to invasion by phytopathogenic microorganisms. *PeerJ* **4**, e1923 (2016).
25. Avenot, H. *et al.* Isolation of 12 polymorphic microsatellite loci in the phytopathogenic fungus *Alternaria brassicicola*. *Molecular Ecology Notes* **5**, 948–950 (2005).
26. Vicente Joana, G. & Holub Eric, B. *Xanthomonas campestris* pv. *campestris* (cause of black rot of crucifers) in the genomic era is still a worldwide threat to brassica crops. *Molecular Plant Pathology* **14**, 2–18 (2012).
27. Verma, P. R., Saharan, G. S. & Canada. Agriculture and Agri-Food Canada. Research Branch. *Monograph on Alternaria diseases of crucifers*. (Ottawa: Research Branch, Agriculture and Agri-Food Canada, 1994).
28. Maude, R. B. *Seedborne diseases and their control: principles and practice*. (1996).
29. Pochon, S. *et al.* The Arabidopsis thaliana-alternaria brassicicola pathosystem: a model interaction for investigating seed transmission of necrotrophic fungi. *Plant Methods* **8**, (9 May 2012)–(9 May 2012) (2012).
30. Wolf, J. M., van der Zouwen, P. Svander & Heijden, L. van der. Flower infection of *Brassica oleracea* with *Xanthomonas campestris* pv. *campestris* results in high levels of seed infection. *Eur J Plant Pathol* **136**, 103–111 (2013).
31. Dembélé, D. & Kastner, P. Fold change rank ordering statistics: a new method for detecting differentially expressed genes. *BMC Bioinformatics* **15**, 14 (2014).
32. Climer, S. *et al.* A Custom Correlation Coefficient (CCC) Approach for Fast Identification of Multi-SNP Association Patterns in Genome-Wide SNPs Data. *Genetic epidemiology* **38**, (610–621 (2014).
33. Garcia, B. J. *et al.* Phytobiome and transcriptional adaptation of *Populus deltoides* to acute progressive drought and cyclic drought. *Phytobiomes*. <https://doi.org/10.1094/PBIOMES-04-18-0021-R> (2018)
34. Lukjancenko, O., Wassenaar, T. M. & Ussery, D. W. Comparison of 61 sequenced *Escherichia coli* genomes. *Microb. Ecol.* **60**, 708–720 (2010).
35. Rezki, S. *et al.* Assembly of seed-associated microbial communities within and across successive plant generations. *Plant Soil* **422**, 67–79 (2018).
36. Torres-Cortés, G. *et al.* Functional microbial features driving community assembly during seed germination and emergence. *Front Plant Sci* **9**, 902 (2018).
37. Klaedtke, S. *et al.* Terroir is a key driver of seed-associated microbial assemblages. *Environ Microbiol* **18**, 1792–1804 (2016).
38. Lopez-Velasco, G., Carder, P. A., Welbaum, G. E. & Ponder, M. A. Diversity of the spinach (*Spinacia oleracea*) spermosphere and phyllosphere bacterial communities. *Fems Microbiology Letters* **346**, 146–154 (2013).
39. Links, M. G. *et al.* Simultaneous profiling of seed-associated bacteria and fungi reveals antagonistic interactions between microorganisms within a shared epiphytic microbiome on Triticum and Brassica seeds. *The New phytologist* **202**, 542–53 (2014).
40. Yang, L. *et al.* Dominant groups of potentially active bacteria shared by barley seeds become less abundant in root associated microbiome. *Front. Plant Sci.* **8** (2017).
41. Terrasson, E. *et al.* Identification of a molecular dialogue between developing seeds of *Medicago truncatula* and seedborne xanthomonads. *Journal of Experimental Botany*, doi:10.1093/jxb/erv167 (2015).
42. Terras, F. R. G. *et al.* Small cysteine-rich antifungal proteins from radish - their rôle in host-defense. *Plant Cell* **7**, 573–588 (1995).
43. Meldau, S., Erb, M. & Baldwin, I. T. Defence on demand: mechanisms behind optimal defence patterns. *Ann. Bot.* **110**, 1503–1514 (2012).
44. Leprince, O., Pellizzaro, A., Berriri, S. & Buitink, J. Late seed maturation: drying without dying. *J Exp Bot* **68**, 827–841 (2017).
45. Niu, B., Paulson, J. N., Zheng, X. & Kolter, R. Simplified and representative bacterial community of maize roots. *Proc. Natl. Acad. Sci. USA* **114**, E2450–E2459 (2017).
46. Barret, M. *et al.* Emergence Shapes the Structure of the Seed Microbiota. *Applied and Environmental Microbiology* **81**, 1257–1266 (2015).
47. Nelson, E. B. Microbial dynamics and interactions in the spermosphere. *Annual Review of Phytopathology* **42**, 271–309 (2004).
48. Hibbing, M. E., Fuqua, C., Parsek, M. R. & Peterson, S. B. Bacterial competition: surviving and thriving in the microbial jungle. *Nat. Rev. Microbiol.* **8**, 15–25 (2010).
49. Fukami, T. Historical Contingency in Community Assembly: Integrating Niches, Species Pools, and Priority Effects. *Annual Review of Ecology, Evolution, and Systematics* **46**, 1–23 (2015).
50. Jacques, M.-A. *et al.* Using Ecology, Physiology, and Genomics to Understand Host Specificity in *Xanthomonas*. *Annu Rev Phytopathol* **54**, 163–187 (2016).
51. Schmidt, C. S., Alavi, M., Cardinale, M., Müller, H. & Berg, G. *Stenotrophomonas rhizophila* DSM14405^T promotes plant growth probably by altering fungal communities in the rhizosphere. *Biol Fertil Soils* **48**, 947–960 (2012).
52. Nelson, E. B. The seed microbiome: Origins, interactions, and impacts. *Plant Soil* **422**, 7–34 (2018).
53. Bai, Y. *et al.* Functional overlap of the Arabidopsis leaf and root microbiota. *Nature* **528**, 364–369 (2015).
54. Martin, M. Cutadapt removes adapter sequences from high-throughput sequencing reads. *EMBnet journal* **17**, 10–12 (2011).
55. Langmead, B. & Salzberg, S. L. Fast gapped-read alignment with Bowtie 2. *Nature methods* **9**, 357–9 (2012).
56. Belmas, E. *et al.* Genome Sequence of the Necrotrophic Plant Pathogen *Alternaria brassicicola* Abra43. *Genome Announc.* **6**, e01559–17 (2018).
57. Wood, D. E. & Salzberg, S. L. Kraken: ultrafast metagenomic sequence classification using exact alignments. *Genome Biology* **15**, R46 (2014).
58. McMurdie, P. J. & Holmes, S. phyloseq: An R Package for Reproducible Interactive Analysis and Graphics of Microbiome Census Data. *PLOS ONE* **8**, e61217 (2013).
59. Peng, Y., Leung, H. C. M., Yiu, S. M. & Chin, F. Y. L. IDBA-UD: a *de novo* assembler for single-cell and metagenomic sequencing data with highly uneven depth. *Bioinformatics* **28**, 1420–1428 (2012).
60. Chin, C.-S. *et al.* Nonhybrid, finished microbial genome assemblies from long-read SMRT sequencing data. *Nat Meth* **10**, 563–569 (2013).
61. Seemann, T. Prokka: rapid prokaryotic genome annotation. *Bioinformatics* **30**, 2068–2069 (2014).
62. Buchfink, B., Xie, C. & Huson, D. H. Fast and sensitive protein alignment using DIAMOND. *Nat Meth* **12**, 59–60 (2015).
63. Huerta-Cepas, J. *et al.* eggNOG 4.5: a hierarchical orthology framework with improved functional annotations for eukaryotic, prokaryotic and viral sequences. *Nucleic Acids Res* **44**, D286–D293 (2016).
64. Li, H. *et al.* The Sequence Alignment/Map format and SAMtools. *Bioinformatics* **25**, 2078–2079 (2009).
65. van Dongen, S., Abreu-Goodger, C. & Using, M. C. L. to extract clusters from networks. *Methods Mol. Biol.* **804**, 281–295 (2012).
66. Kang, D. D., Froula, J., Egan, R. & Wang, Z. MetaBAT, an efficient tool for accurately reconstructing single genomes from complex microbial communities. *PeerJ* **3**, e1165 (2015).
67. Parks, D. H., Imelfort, M., Skennerton, C. T., Hugenholtz, P. & Tyson, G. W. CheckM: assessing the quality of microbial genomes recovered from isolates, single cells, and metagenomes. *Genome Res.* **25**, 1043–1055 (2015).
68. Richter, M. & Rosselló-Móra, R. Shifting the genomic gold standard for the prokaryotic species definition. *Proc. Natl. Acad. Sci. USA* **106**, 19126–19131 (2009).

69. Luo, R. *et al.* SOAPdenovo2: an empirically improved memory-efficient short-read de novo assembler. *Gigascience* **1**, 18 (2012).
70. Zerbino, D. R. & Birney, E. Velvet: Algorithms for de novo short read assembly using de Bruijn graphs. *Genome Res.* **18**, 821–829 (2008).
71. Callahan, B. J. *et al.* DADA2: High-resolution sample inference from Illumina amplicon data. *Nature Methods* **13**, 581–583 (2016).
72. Glassner, H. *et al.* Bacterial niches inside seeds of *Cucumis melo* L. *Plant Soil* **422**, 101–113 (2018).
73. Amann, R. I. *et al.* Combination of 16S rRNA-targeted oligonucleotide probes with flow cytometry for analyzing mixed microbial populations. *Appl. Environ. Microbiol.* **56**, 1919–1925 (1990).
74. Daims, H., Brühl, A., Amann, R., Schleifer, K.-H. & Wagner, M. The Domain-specific Probe EUB338 is Insufficient for the Detection of all Bacteria: Development and Evaluation of a more Comprehensive Probe Set. *Systematic and Applied Microbiology* **22**, 434–444 (1999).
75. Darrasse, A., Barret, M., Cesbron, S., Compant, S. & Jacques, M.-A. Niches and routes of transmission of *Xanthomonas citri* pv. *fuscans* to bean seeds. *Plant Soil* **422**, 115–128 (2018).
76. Günter, W., Rudolf, A. & Wolfgang, B. Optimizing fluorescent *in situ* hybridization with rRNA-targeted oligonucleotide probes for flow cytometric identification of microorganisms. *Cytometry* **14**, 136–143 (1993).

Acknowledgements

The authors wish to thank Guillaume Chesneau for his help with bacterial competition assays, Laurent Noel for providing the strain *pTac::GUS-GFP*, the FNAMS for running field experiments, the ANAN platform (SFR QuaSav) for amplicon sequencing and BGI for sequencing the bacterial genomes. We would also like to thank BBRIC network for all the bioinformatic support. This research was supported by the grant awarded by the Region des Pays de la Loire (metaSEED, 2013 10080); RFI Objectif Végétal (DynaSeedBiome) and the AgreeSkills + fellowship programme, which has received funding from the EU's Seventh Framework Programme under grant agreement n° FP7-609398. This research used resources from the Oak Ridge Leadership Computing Facility at the Oak Ridge National Laboratory, which is supported by the Office of Science of the U.S. Department of Energy under Contract No. DE-AC05-00OR22725. This research was also supported by the Plant-Microbe Interfaces Scientific Focus Area in the Genomic Science Program, the Office of Biological and Environmental Research (BER) in the U.S. Department of Energy Office of Science, and by the Department of Energy, Laboratory Directed Research and Development funding (ProjectID 8321).

Author Contributions

G.T.C., B.G., S.C., D.J. and M.B. designed the study and made substantial contributions to the analysis and interpretation of the results. G.T.C., B.G., J.P. and M.Br. carried out bioinformatic analyses and participated actively in the interpretation of the results. S.C. performed F.I.S.H. analyses. S.R. and A.P. performed all the microbiological analyses and Biolog profiles. A.R. and O.B. carried out the HiSeq and PacBio sequencing of the environmental DNA. G.T.C., B.G. and M.B. wrote the manuscript with input from the other authors. All authors read and approved the final manuscript.

Additional Information

Supplementary information accompanies this paper at <https://doi.org/10.1038/s41598-019-42865-9>.

Competing Interests: The authors declare no competing interests.

Publisher's note: Springer Nature remains neutral with regard to jurisdictional claims in published maps and institutional affiliations.



Open Access This article is licensed under a Creative Commons Attribution 4.0 International License, which permits use, sharing, adaptation, distribution and reproduction in any medium or format, as long as you give appropriate credit to the original author(s) and the source, provide a link to the Creative Commons license, and indicate if changes were made. The images or other third party material in this article are included in the article's Creative Commons license, unless indicated otherwise in a credit line to the material. If material is not included in the article's Creative Commons license and your intended use is not permitted by statutory regulation or exceeds the permitted use, you will need to obtain permission directly from the copyright holder. To view a copy of this license, visit <http://creativecommons.org/licenses/by/4.0/>.

© The Author(s) 2019